

This is a repository copy of *Investigating the stability and degradation of hydrogen PEM fuel cell*.

White Rose Research Online URL for this paper:

<https://eprints.whiterose.ac.uk/id/eprint/178138/>

Version: Accepted Version

---

**Article:**

Dhimish, Mahmoud, Vieira, Romênia G. and Badran, Ghadeer (2021) Investigating the stability and degradation of hydrogen PEM fuel cell. *International Journal of Hydrogen Energy*. pp. 37017-37028. ISSN: 0360-3199

<https://doi.org/10.1016/j.ijhydene.2021.08.183>

---

**Reuse**

This article is distributed under the terms of the Creative Commons Attribution-NonCommercial-NoDerivs (CC BY-NC-ND) licence. This licence only allows you to download this work and share it with others as long as you credit the authors, but you can't change the article in any way or use it commercially. More information and the full terms of the licence here: <https://creativecommons.org/licenses/>

**Takedown**

If you consider content in White Rose Research Online to be in breach of UK law, please notify us by emailing [eprints@whiterose.ac.uk](mailto:eprints@whiterose.ac.uk) including the URL of the record and the reason for the withdrawal request.

# Investigating the Stability and Degradation of Hydrogen PEM Fuel Cell

Mahmoud Dhimish<sup>1</sup>, Romênia G. Vieira<sup>2</sup> and Ghadeer Badran<sup>1</sup>

<sup>1</sup> Department of Electronic Engineering, University of York, York YO10 5DD, UK

<sup>2</sup> Department of Engineering and Technology, Semi-Arid Federal University,  
Francisco Mota Av., Mossoro 59625-900, Brazil

## **Abstract**

The hydrogen proton exchange membrane (PEM) fuel cells are promising to utilize fuel cells in electric vehicle (EV) applications. However, hydrogen PEM fuel cells are still encountering challenges regarding their functionality and degradation mechanism. Therefore, this paper aims to study the performance of a 3.2 kW hydrogen PEM fuel cell under accelerated operation conditions, including varying fuel pressure at a level of 0.1 to 0.5 bar, variable loading, and short-circuit contingencies. We will also present the results on the degradation estimation mechanism of four fuel cells working at different operational conditions, including high-to-low voltage range and high-to-low temperature variations. These experiments examine over 180 days of continuous fuel cell working cycle. We have observed that the drop in the fuel cells' efficiency is at around 7.2% when varying the stack voltage and up to 14.7% when the fuel cell's temperature is not controlled and remained at 95°C.

**Keywords:** Fuel cell degradation; Fuel cell performance under ramp pressure; CDF model for fuel cell degradation; Fuel cell performance under purging routines.

## **1. Introduction**

Fuel cells are electromechanical devices that convert the chemical energy stored in a fuel (*i.e.*, hydrogen) directly into electrical energy that can be utilized with DC or AC applications. Hence, fuel cells are a form of a clean source of energy. Besides, fuel cell systems comprise a wide range of sub-systems, including the fuel cell stack, auxiliary units such as a cooling circuit, an air compressor, and a DC-DC converter. All of these components are checked/maintained using the internal control processing unit. Industrial gas supply, rocket industry, electric vehicles (EV), jet airplanes, portable devices, and trains are examples of the current commercial-off-the-shelf applications for fuel cells.

Accordingly, this section aims to (i) present the research background in this field, including existing fuel cells technologies, and (ii) discuss our contributions to knowledge.

## 1.1 Literature Review

Several industrial-based fuel cell applications use the proton exchange membrane (PEM) fuel cells since they provide high-efficiency energy conversion, moderately with minimal pollutant emissions and a silent operation mechanism. These features render the critical driving force behind PEM usage in today's market.

In the last couple of years, scholars started to analyze PEM fuel cells' operational behavior using real-time simulation procedures described by Sagar *et al.* [1]. Also, as Khalid *et al.* [2] suggested, simulation analysis is not competent when integrating fuel cells with actual hardware-in-the-loop applications, such as when connected with smart microgrids and EV applications. Adopting a multi-layer control procedure can mitigate this problem within the fuel cell-based application, such as the disturbance-observed-based control model developed by Liu *et al.* [3] or the single inductor self-start up energy combiner circuit proposed by Umaz [4].

Hence, the optimization models, particularly for PEM fuel cells, are fundamental to be considered if there were no control processing unit, as we understand from the low-cost commercial-off-the-shelf fuel cells [5]. Besides, the optimization models must have the ability to monitor the fuel cell's behaviour and working cycles, as was advised by the new online self-cold start-up methodology developed by Amamou *et al.* [6] and the hierarchical management control-based methods [7].

The conventional configuration of a fuel cell based EV application is demonstrated in Fig. 1. In this arrangement, the fuel cell must comprise a control system (with stability mode controller) to connect quickly and control the fuel cell's current flow into the DC-DC converter, followed by a DC-AC inverter linked with the wheel drive machinery. Here, the DC-DC converter must act unidirectional, where no feedback/reversed current passes into the fuel cell [8, 9].

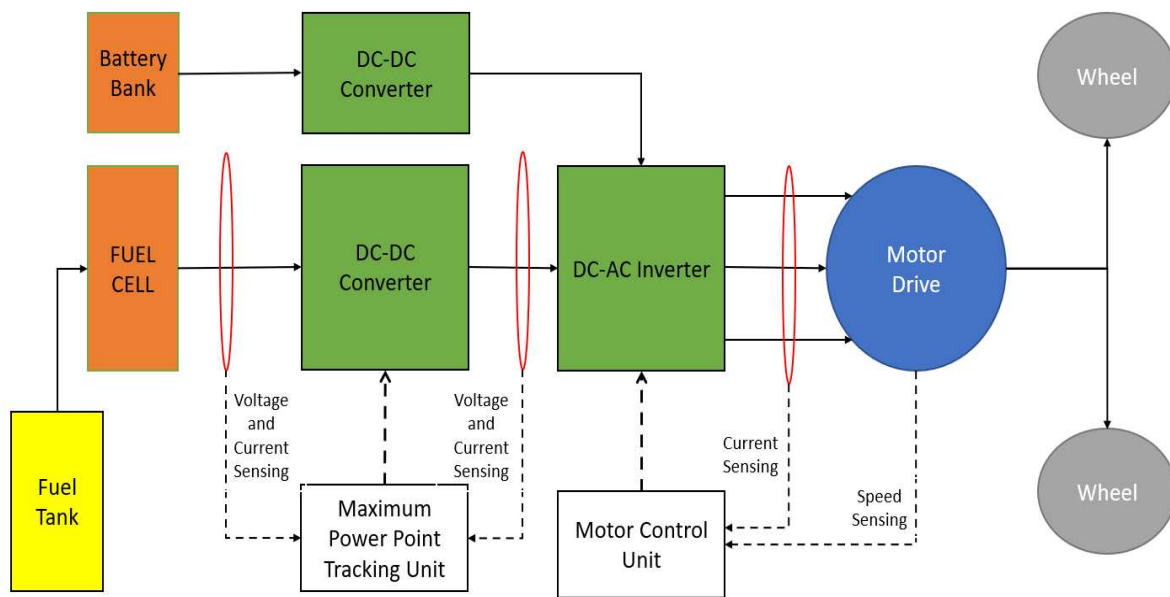


Fig. 1. Conventional configuration of fuel cell-based EV application.

It is also worth noting that current fuel cell EV models follow the configuration as in Fig. 1. The problem arises when the voltage produced by the fuel cell is insufficient due to the low loading [10]. This problem became of the current challenges in today's fuel cell application as it is still challenging to explain how this mechanism degrade the fuel cell performance over time.

Several scientists have discussed the drop in the fuel cell's output voltage; however, with an insignificant in-depth perception of its short-circuit states, which could be the source of this problem. As of example, Umza [11] has described power management in low-voltage fuel cell application; a similar study was also represented by [12] and [13]. However, the low-voltage operation did not crave the actual drop in the tested PEM fuel cells while running under short-circuit conditions.

Recently it was discovered that using novel operational adaptability control methods can optimize the voltage regulation of PEM fuel cells, as described by Bankupalli *et al.* [14]. Although, these methods only apply to optimized-based fuel cells that have no control processing units. Besides, the neuro-fuzzy inference system (ANFIS) developed by Liu *et al.* [15] can improve PEM fuel cells' short-term prognostics but abandon operating under short-circuit or high-temperature variations.

Additionally, the obstruction of fuel cell integration with renewable energy resources and micro-grids is the lack of understanding of the fuel cell performance and characterization whistle working under varying fuel pressure (measured in bar). We have seen the characterization using the hardware-in-the-loop testing for fuel cells in [16-18], yet the actual energy conversion efficiency under varying pressure was unevaluated. This aspect kept many industrial forms apart from the integration of fuel cells inside their remits.

In addition to the abovementioned literature, fuel cells' reliability and degradation have been inconsiderably reported [18]. An exciting work by Javaid *et al.* [19] and Pregelj *et al.* [20] have remarked that there might be a linkage of fuel cell degradation due to short-circuit cycling (when not enough voltage is produced by the fuel cell) and an increase in the membrane temperature. It was also observed that the fuel cells' energy conversion efficiency is also expected to drop in both conditions. Their actual investigation was made using short-term data measurement (less than 1-day).

The reliability analysis, such as degradation estimation, for fuel cells is vital to investigate, particularly when it comes to integrating fuel cells with the power grid and when a hybrid renewable energy source and integrable within a micro-grid infrastructure. For example, in [21], authors have presented a brief assessment of the energy management of reconfigurable residential intelligent hybrid AC/DC microgrids considering a combination of heat and power loads and electric vehicles charging/discharging points. Interestingly, they found that minor variations in the system's efficiency can lead to heavy drop/cut-down; for example, this applies when connecting a fuel cell into the micro-grid and operating under high-temperature levels. In addition, this cut down in micro-grids could also be the case when the fuel cells are working under low voltages (below the internal DC/DC converter) [22].

For that reason, optimal operation and energy management of a grid-connected fuel cell-based system must be obtained. This topic has been widely investigated because of its significance. For example, in [23], an optimal design of the operational grid-connected fuel cell using particle swarm optimization was presented. Their results show that the grid-connected fuel cell-based combine heat and power (CHP) system causes lower operating costs in the near future. On the other hand, Mohamed *et al.* [24] have presented a novel fuzzy-based cloud stochastics framework for renewable microgrids' energy management based on maximum deployment of electric vehicles and fuel cell integration. They found that using the fuzzy-based model can improve the performance by optimizing the system costs at different operational scenarios, i.e., when increasing or decreasing the capacity of the fuel cell, 30 - 200 kW.

The co-production of electricity and hydrogen from wind was investigated by Rezaei *et al.* [25]. They have summarised a wide range of scenarios and found that fuel cell-based systems can make a massive step towards reducing electricity costs. Still, they have insisted that estimating the reliability of these new technologies must be further contemplated. As an example of fuel cell reliability analysis, in 2021, multiscale modelling of degradation of full solid oxide fuel cell stacks has been presented in [26]. The model simulated 38 thousand fours of the stack life in 1 h and 15 minutes. In contrast, Hahn *et al.* [27] have present the optimization of the efficiency (increased by 3.5%) and degradation rate (reduced by 2%) for an automotive fuel cell system. In addition, a similar study was presented by [28] on the dynamic reliability assessment of PEM fuel cell systems using only simulation measurements. They claim that fuel cell systems are likely to fail after 4000 working hours.

## **1.2 Paper Contributions and Organization**

In the previous section, we have demonstrated that there is currently a lack of experimentation activity on fuel cell's performance and degradation mechanism. Therefore, this article aims to present how PEM-type fuel cells perform under ramp pressure variations, purging routines and empirically evaluate the degradation of different fuel cells functioning under various conditions, including a set of the output voltage and temperature variations. Specifically, we will conduct the experiments using a 3.2 KW fuel cell used for EV application and observed a significant drop (15%) in the output power conversion efficiency when varying the H<sub>2</sub> pressure from 0.1 to 0.5 bar. We will also demonstrate that if the membrane temperature increases from 50 to 95°C for the same fuel cell type, the efficiency is expected to drop from 47.78% to 33.13%. Such experiments enable evaluating the fuel cell behaviour under different operational conditions and assessing the performance results for about 180 days of the working cycle.

This article is organised as follows: Section 2 will present the examined fuel cell operation. In contrast, in Section 3, the characteristics of the fuel cell will be discussed. Then, section 4 explains the work examined on degradation estimation of the fuel cell performance. Last Sections 5 and 6 will demonstrate the comparative study and conclusions, respectively.

## 2. Examined Fuel Cell Characteristics

This section spans two objectives, (i) present the examined fuel cell prototype and its characteristics, (ii) discuss the fuel cell testing facility.

### 2.1 Description of the Fuel Cell Prototype

In this work, we have examined a 3.2 kW fuel cell manufactured by MES-DEA, applied for EV; this fuel cell has been widely used by Toyota and other EV cars available in today's market. The physical layout of the fuel cell is shown in Fig. 2.

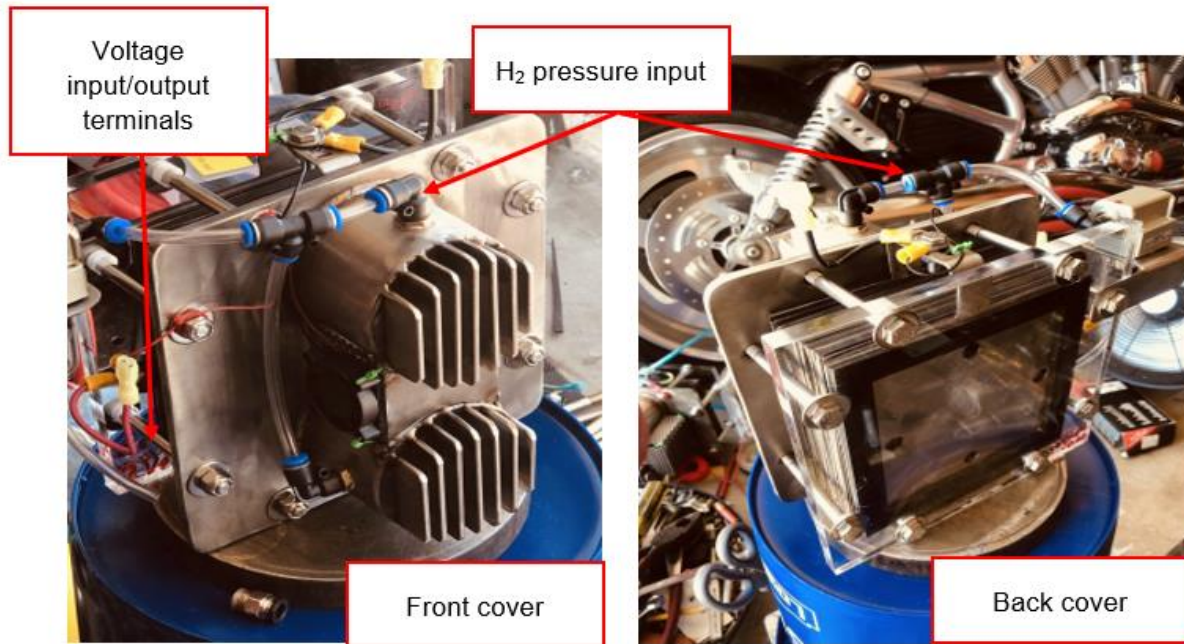


Fig. 2. Examined MES-DEA 3.2 kW fuel cell

This fuel cell is composed to be lightweight and has simplistic operating conditions. The fuel cell has two stacks, each comprising 60 series-connected cells, and it has an active area of 60 cm<sup>2</sup>. Concerning the fuel cell's air-cooling mechanism, each stack has its separate air-cooling operation under ambient pressure.

This fuel cell has a DC output voltage range of 72 to 120 V, depending on the applied pressure and load variations. So, its typical application is to drive the engine/motor of the EV.

Table I presents a comprehensive summary of both the fuel cell performance and its operating conditions. We can notice that the fuel cell can relatively operate at a high temperature, 75°C. Applying a 0.3 bar of pressure to the cell to function at its optimum working cycle, with minimal degradation *versus* time, is recommended. The maximum applied H<sub>2</sub> pressure can be fixed at 0.5 bar. Thus, a continuous working process can still be possible from 0.1 to 0.5 bar.

## Fuel Cell Performance

Examined Fuel Cells Characteristics	
Fuel Cell Performance	
DC Output Voltage Range	72 to 120 V
Maximum Rater Power	3.2 kW
Maximum Power Dissipation	325 W
Total Number of Cells	120
Active Cell Area	60 cm <sup>2</sup>
Fuel Cell Operating Conditions	
Maximum Operating Temperature	75 °C
Nominal H <sub>2</sub> Pressure	0.3 bar
Maximum/overload H <sub>2</sub> Pressure	0.5 bar
Air Pressure	Ambient
Fuel Supply	Pure Hydrogen
Control System Requirement	12 V input
Weight	10 kg
Cooling System Requirements	12 V input
Working Cycle	Continuous Mode
Gas Humidification	None

The cell's fuel supply is pure (99.99%) hydrogen; most importantly, it has no auxiliary hydration plant and a simplified humidification process involved in its working cycle. A control signal is sent to a humidity exchanger to compensate for the cell's humidity level. An air compressor is also operated during this process; see Fig. 3 for the fuel cell system's simplified schematic.

Both cooling and control system requirement is 12 V, can be supplied separately from an internal buck DC-DC converter placed in the fuel cell controller unit. Both internal processing units have a limited power dissipation, ranging from 45 to 425 W. A serial communication port is also available in this fuel cell, establishing an easy digital signal process of relevant parameters to be continually monitored/checked.

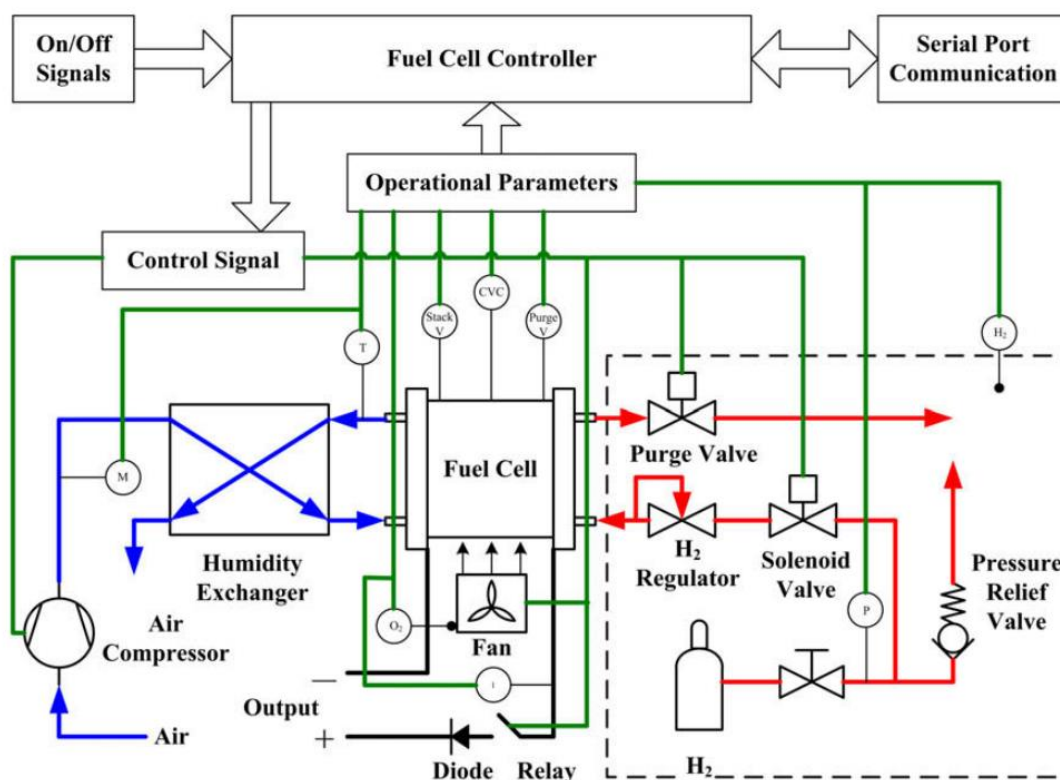


Fig. 3. Detailed schematic of the fuel cell system.



It is worth realizing that the fuel cell membranes must be kept hydrated for the fuel cell's water management. Otherwise, the reaction process would be diminished, resulting in (i) damage of failure in the cell, in the worst-case scenario, a short-circuit condition could occur, or (ii) increasing the membrane resistance, hence, leading to a significant drop in the output regulated voltage.

In the examined fuel cell, the stack is systematically purged via the control system, opening the air valve, thus supplying fresh air, subsequently draining the excess water accumulated during the reaction process. This programmable process is performed every 30s for a complete duration of 1s. This process is also monitored using the airflow meter.

Besides, to keep a certain hydration level, the stack is electronically short-circuited for 1s every 30s. This operation is activated by the fuel cell's internal MOSFET devices to maintain sufficient water in the stacked membrane and nurture its moisture level.

## **2.2 Fuel Cell Testing Facility**

A testing facility was assembled to test and categorize the examined fuel cell's effectiveness under varying conditions. The fuel cell requires near pure, 99.99% hydrogen gas at a typical gauge pressure of 0.3 bar, maximum 0.5 bar. The maximum flow rate also has to be retained below 65 l/min. A compressed hydrogen gas, 175 bars, is also stored in the laboratory for the testing phase, as shown in Fig. 4(a). Overpressure safety vents, drainage pints, and ventilation fans were also installed for health and safety requirements.

A pressure transducer (WIKA model) with an integrated controllable value supported the experimental work. The pressure can be regulated electronically, from 0 to 5 bar. Voltage and current transducers (HAS 100-s model) were also used to measure the fuel cell stack and load variations.

The fuel cell test chamber is shown in Figure 4(b). The fuel cell is connected with a pure controllable resistive load bank, while the gas and electrical instruments are placed inside the fuel cell test chamber. The data acquisition was developed using National Instrument (NI) DAQ 6008 model and combined with a personal computer to collect related data.

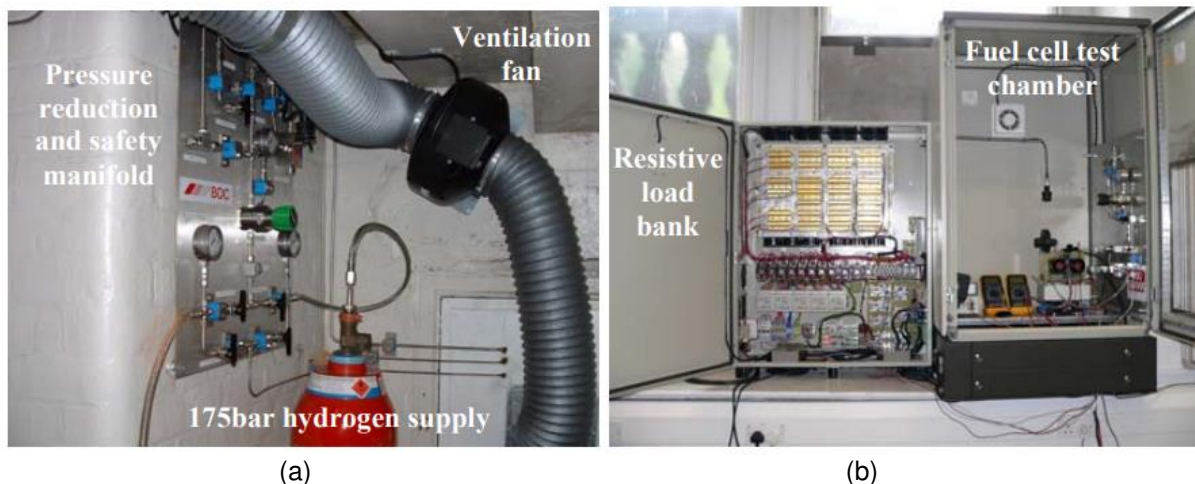


Fig. 4. Testing facility (a) hydrogen supply and pressure control, (b) fuel cell testing chamber and the resistive load bank.



### 3. Results

#### 3.1 Fuel Cell Output Characteristics

The examined fuel cell was experimented with the variable resistive load to investigate its performance. The loading conditions were also repeated by varying the H<sub>2</sub> pressure from 0.1 to 0.5 bar. As shown earlier in Table I, the recommended H<sub>2</sub> pressure to set is at 0.3 bar.

The output voltage-current characteristics of the fuel cell are presented in Fig. 5(a). Increasing the H<sub>2</sub> pressure would increase the output voltage at full load current, 35A. The minimum output regulated voltage varies from 80 to 61 V, under 0.5 and 0.1 bar, respectively. Besides, at the no-load condition, 0 A, the output voltage is equivalent to 119 V in all H<sub>2</sub> pressure variations.

When increasing the H<sub>2</sub> pressure of the fuel cell, as shown in Fig. 5(b), the output power increases. The maximum output power is obtained when a full load condition is applied equally to 2835 W at 0.5 bar, while at the recommended H<sub>2</sub> pressure, 0.3 bar, the output power is equal to 2625 W. Under moderate load variations, 0.25 A to 10 A, the output power maintains approximately at the same level of 1000W.

In theory, the drop in the output voltage is expected to be linear. However, as we conducted the tests on an actual fuel cell was used for an EV application, the linearity is expected not to be the case. In this example, Figs 5(a) and 5(b), there was a continuous decrease in the output voltage as we increased the current. However, we observed some measurement variations due to the fuel cell degradation and the accuracy ( $\pm 3\%$ ) of the voltage-current testing equipment (Fluke T6-600).

The fuel-to-electrical output conversion efficiency of the fuel cell can be calculated using (1). The output electricity produced by the cell ( $W_{Electricity}$ ) is obtained by simply multiplying the output voltage and current, shown in Fig. 5(b). However,  $W_{H_2}$  is the actual H<sub>2</sub> consumption by the fuel cell measured in J/s (Watts), shown in Fig. 6(a). At full load, as the pressure rise, H<sub>2</sub> consumption is undoubtedly increasing.

$$\eta = \frac{W_{Electricity}}{W_{H_2}} \quad (1)$$

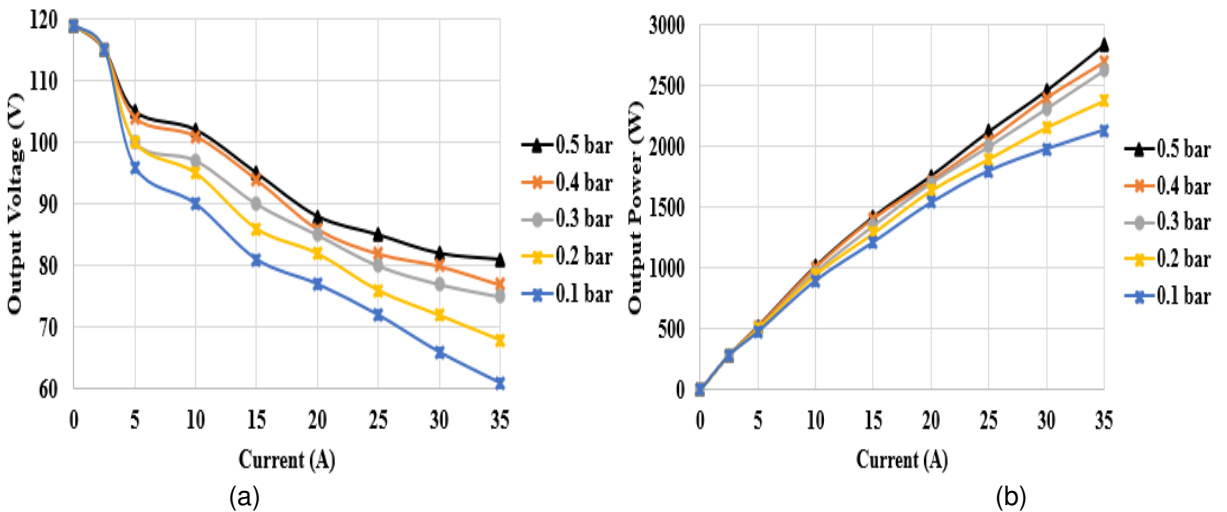


Fig. 5. (a) fuel cell output voltage vs output current, (b) fuel cell output power vs output current, (b) fuel cell efficiency vs load current.

The efficiency of the examined fuel cell is presented in Fig. 6(b). We can observe that the efficiency increases for high-loading conditions (20 A or more) as we raise the H<sub>2</sub> pressure. In the recommended H<sub>2</sub> pressure (0.3 bar), the fuel cell's efficiency at full load is 44%. The fuel cell is expected to have no more than 60% efficiency, even at higher H<sub>2</sub> pressure. In the studied case, the maximum efficiency observed is equal to 58% when the H<sub>2</sub> pressure is fixed at 0.1 bar at an extremely low load condition, 5 A.

Usually, in EV cars, the fuel cell operates at medium-to-high loading [2] and [6], usually above 20 A. Considering this factor, the fuel cell's average efficiency at the recommended operating H<sub>2</sub> pressure equals 47.5%, good enough compared with industrial fuel cells commercially available in today's market.

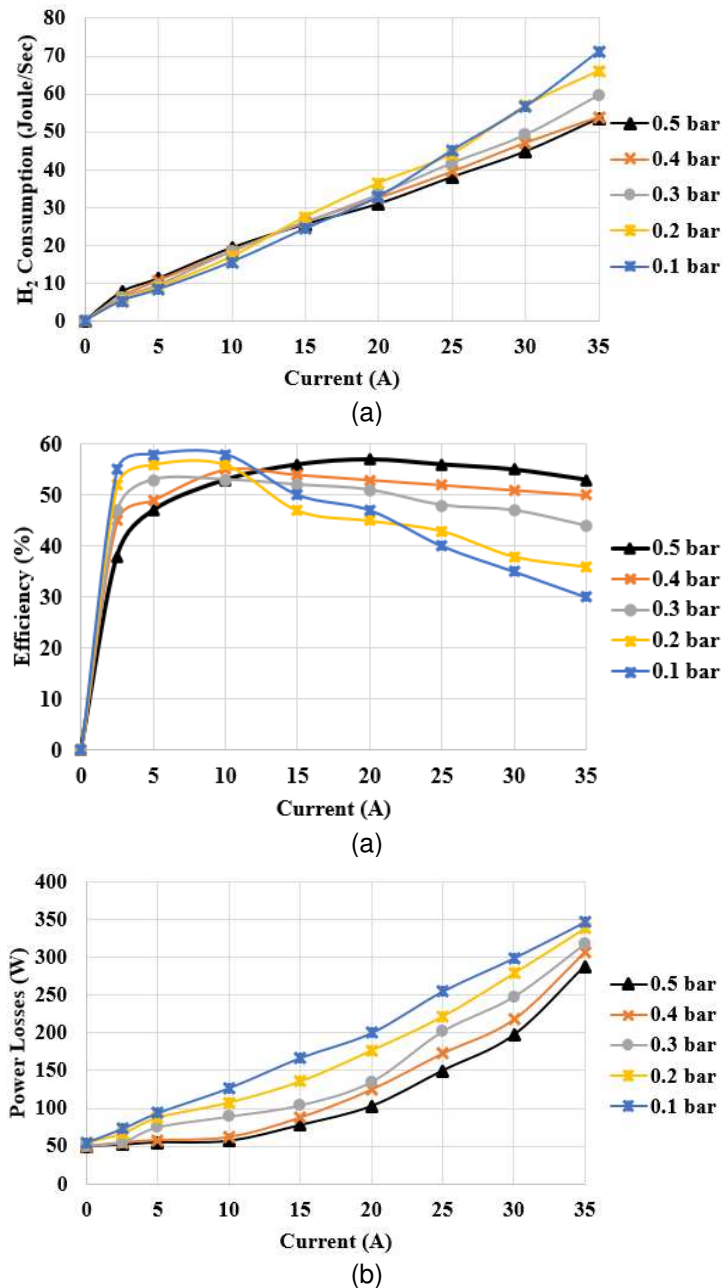


Fig. 6. (a) H<sub>2</sub> consumption, (b) fuel cell efficiency, (c) total power losses in the fuel cell.

There are various reasons for the drop in efficiency; some cannot be eliminated, such as the internal electrochemical system. Nevertheless, we can observe the actual losses of the fuel cell controller, including the operation of the fan and valves. The total power losses have been measured and presented in Fig. 6(c).

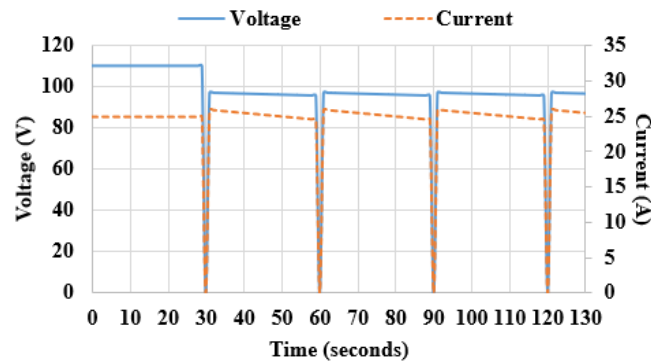
The power losses range from 52 W (no-load condition) to 347 W (full load condition). This result is close to the fuel cell characteristics presented in Table I.

### **3.2 Fuel Cell Output Characteristics at Short-Circuit and Purging Routines**

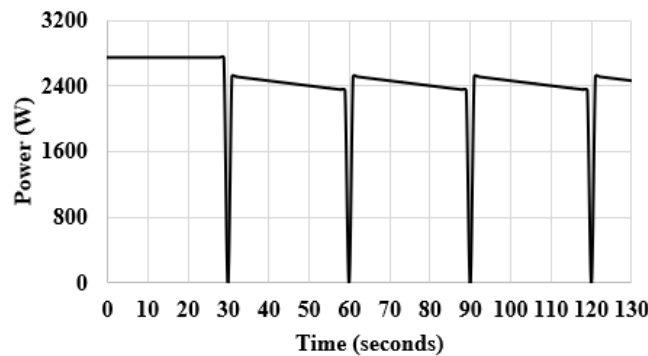
As discussed earlier in Section 2, the fuel cell system is periodically short-circuited and purged (every 30s, for 1s) via the internal control unit to keep the stacked membrane hydrated and release the excess water. This condition occurs only activated when the output voltage falls below 97 V.

We have experimented with the fuel cell under 110 V for 30 s. The sampling rate was rated at one sample per 0.1 s. Suddenly we dropped the load, respectively, the output voltage dropped to 97 V, as shown in Fig. 7(a). Thus, the fuel cell's output voltage and current become zero. It is also clear that every 30 s, while the voltage is still below 97 V, the control unit short-circuited the cell for 1 s (at rigorously 60 s, 90 s, 120 s, etc.).

In contrast, the fuel cell output power is zero during the purging routines, as shown in Fig. 7(b), as no voltage or current is discharged from the fuel cell. In EVs, during fuel cell short-circuited conditions, the battery bank would supply the current to the DC-DC converter and subsequently to the machine/motor. As a result, the purging routines would drop the fuel cell's efficiency and cause degradation in its material; this will be investigated in the next section.



(a)



(b)

Fig. 7. Fuel cell at short-circuit condition (a) output voltage and current, (b) output power.

#### 4. Degradation Estimation of the Fuel Cell

In this section, the degradation estimation of the fuel cell will be investigated under two case studies. As shown in Fig. 8, we have experimented with two fuel cells connected with variable resistive load in the first case study. In the first cell (fuel cell #1), the output voltage is 100 V, while the second (fuel cell #2) is 75 V (below the threshold of 75 V, so purging routines will be demanded). In addition, the temperature is maintained at 50°C, below the threshold of 75°C, as previously shown in Table I.

In the second case study, we evaluated fuel cell #3 and fuel cell #4 under the same output voltage of fuel cell #1 and fuel cell #2, respectively. However, this case study was established to investigate the fuel cell's further degradation at an exhausting temperature at 90°C. It was done by setting the electronic control unit to manage the membrane temperature at this high level.

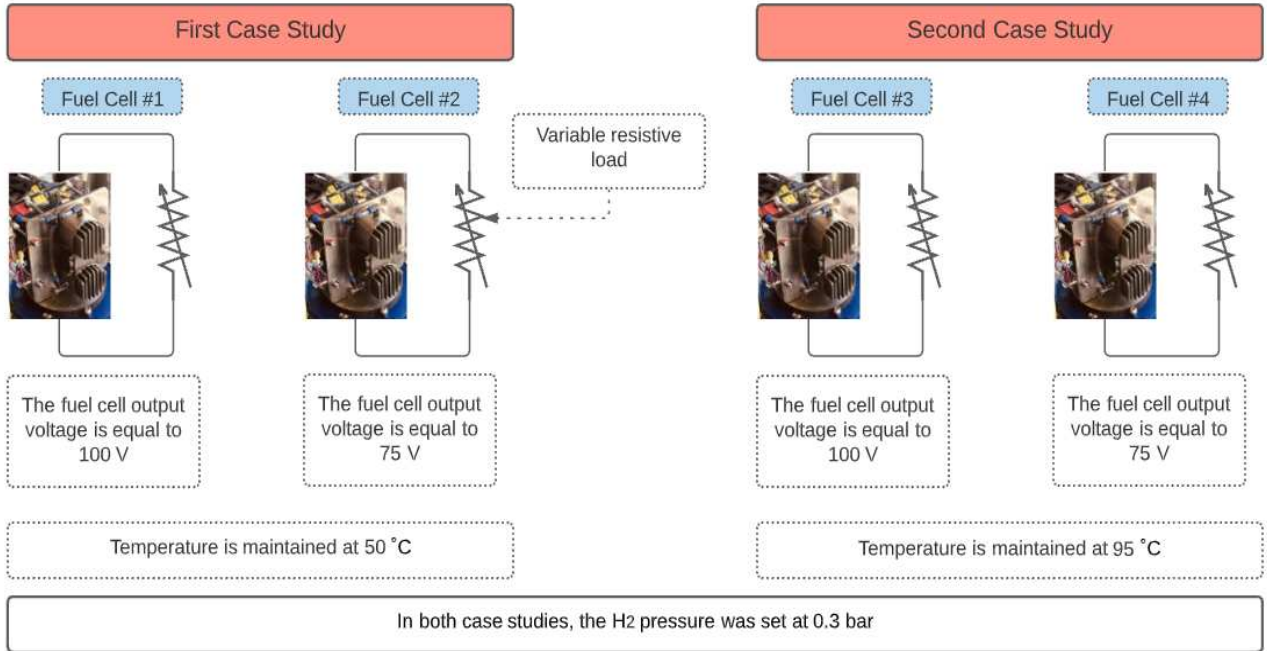


Fig. 8. Experimentation of degradation for the fuel cell under varying voltage regulation and temperature.

Each case study lasts for 180 days; the sampling rate of one sample/hour was averaged. Hence, we have successfully collected 4320 samples for every tested fuel cell. Besides, the H<sub>2</sub> pressure was fixed at 0.3 bar.

According to the first case study, cells #1 and #2's measured efficiency is shown in Fig. 9(a). In addition, we assessed for the 12-days moving average data is also presented, using (2).

$$\text{Moving Average} = \frac{S_1 + S_2 + S_3 + \dots + S_N}{N} \quad (2)$$

where  $S_1$  is the first sample,  $S_N$  is the last sample,  $N$  is the number of samples to be averaged. In our case,  $N = 12$ , suitable to identify the decay of efficiency.

Fuel cell #1 is working under normal conditions, no short-circuit is occurring, and the temperature is below the threshold ( $75^{\circ}\text{C}$ ). There is a minor decay of efficiency to 45% after approximately 1200 hours (50 days). The average efficiency of the cell is 47.78% over the testing period.

Unlike fuel cell #1, the second tested fuel cell #2 operated under 75 V, resulting in a short-circuited condition every 30 s, as demonstrated earlier in Fig. 7. The measured efficiency of fuel cell #2 is shown in Fig. 9(a). The efficiency decay took place after operating for nearly 1104 hours (46 days); it continues until almost reaching a saturation level of 27%. Thus, the average efficiency of the cell is 40.59% over the testing period. This result confirms the reality that short-circuited conditions could cause a significant drop in fuel cell efficiency.

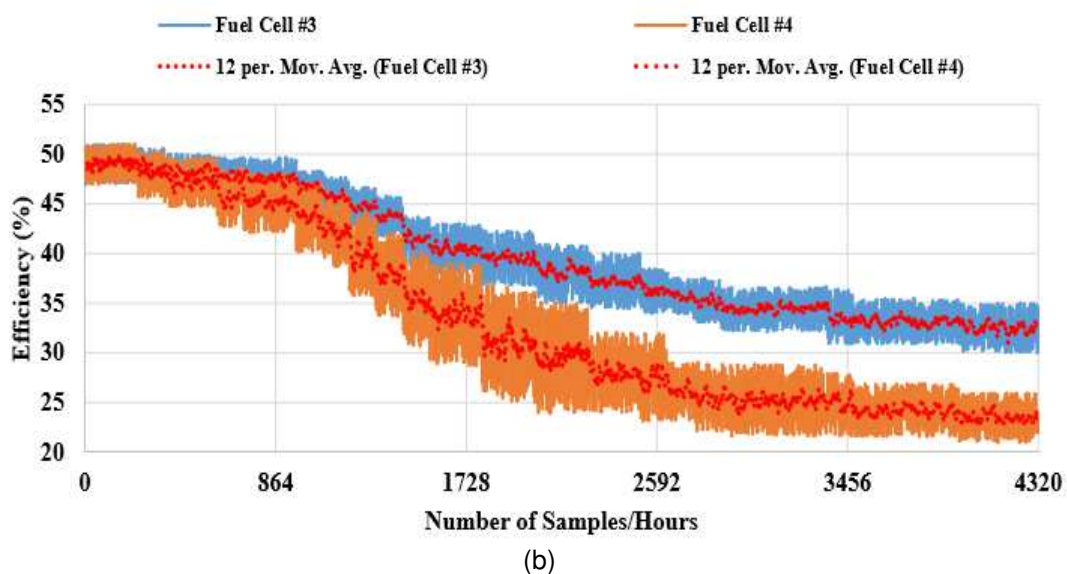
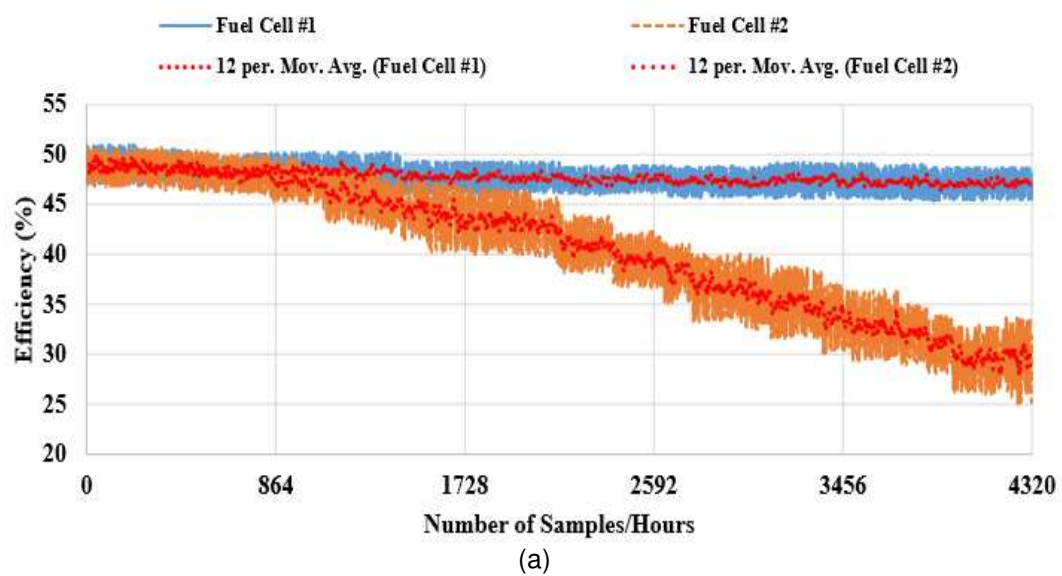


Fig. 9. Output measured efficiency (a) Fuel cells #1 and #2, (b) Fuel cells #3 and #4.

According to the results of fuel cell #3 shown in Fig. 9(b), increasing the temperature of the fuel cells' membrane would reduce its efficiency because of the potential degradation of the cell due to the thermal loading. Having said this, fuel cell #3 is working under 95°C and had an average efficiency of 39.67% over the testing period. The efficiency's saturation level at 33% was achieved after approximately 3456 operational hours (144 days).

A similar result was perceived when testing fuel cell #4, as presented in Fig. 9(b). However, this cell suffers from two conditions, (i) high operating temperature at 95°C and (ii) short-circuit state. The fuel cell started to disfunction nearly after 864 hours (36 days). The efficiency's saturation level at 22% was achieved after approximately 3456 operational hours (144 days). The average efficiency of the cell is 33.13% over the testing period.

Table II demonstrates a summary of the results for the tested fuel cells. The efficiency drops while reducing the voltage due to the short-circuited conditions and increasing the cell's temperature would decrease efficiency.

No. Fuel Cell	Operating Voltage (V)	Membrane Temperature (°C)	Average Efficiency after 180 days (%)
#1 (normal operation)	100	50	47.78
#2	75	50	40.59
#3	100	95	39.67
#4	75	95	33.13

In probability theory and statistics, the cumulative distribution function (CDF) profile presents the relationship between the variable (in our example, fuel cell efficiency) and the probability of occurrence (estimated in %). The CDF profiles of the tested fuel cells are shown in Fig. 10(a). As recommended in [29, 30], it is statistically recommended not to take high probability (*i.e.*, 90%) or low probability (*i.e.*, 10%) while dealing with variables efficiency standards. Hence, in our case, we took the intermediate range of 50%.

There is a 50% chance that a fuel cell working under normal operation mode (fuel cell #1) has a 46.7% efficiency. While for fuel cells working at short-circuited conditions, the expected efficiency is 40.6%. When a fuel cell operating at high-voltage and high-temperature, it is expected, with a chance of probability of 50%, that the cell's efficiency is equal to 39.7%. While under worst-case conditions, when a fuel cell operating under short-circuit and high-temperature conditions, the efficiency is expected to be 33.2%. When a fuel cell runs at high-voltage and high-temperature, it is expected with a chance of probability of 50% that the cell's efficiency is equal to 39.7%. Under worst-case conditions, when a fuel cell operates under short-circuit and high temperature, the efficiency is expected to be 33.2%. It is worth noting that all the CDF results are matching with the averaged results in Table II.



We can also compare the fuel cells' performance using the Dendrogram analysis as presented in Fig. 10(b). There is a similar significant rate (98.5%) between fuel cells #2 and #3. Even though both are working in different operating conditions, the measured efficiency decay following the same pattern. Both cells are 92% similar to fuel cell #1, which works under normal operating conditions.

Interestingly, a flatter similarity rate (72.22%) was observed between cells #1, #2, and #3 and cell #4. It occurs because fuel cell #4 is running under worst-case conditions.

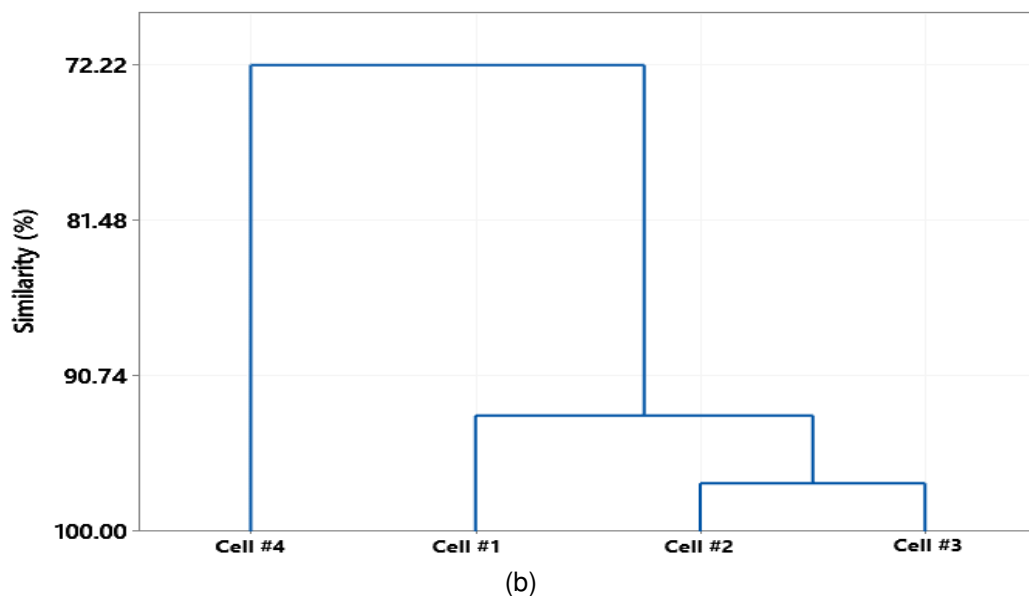
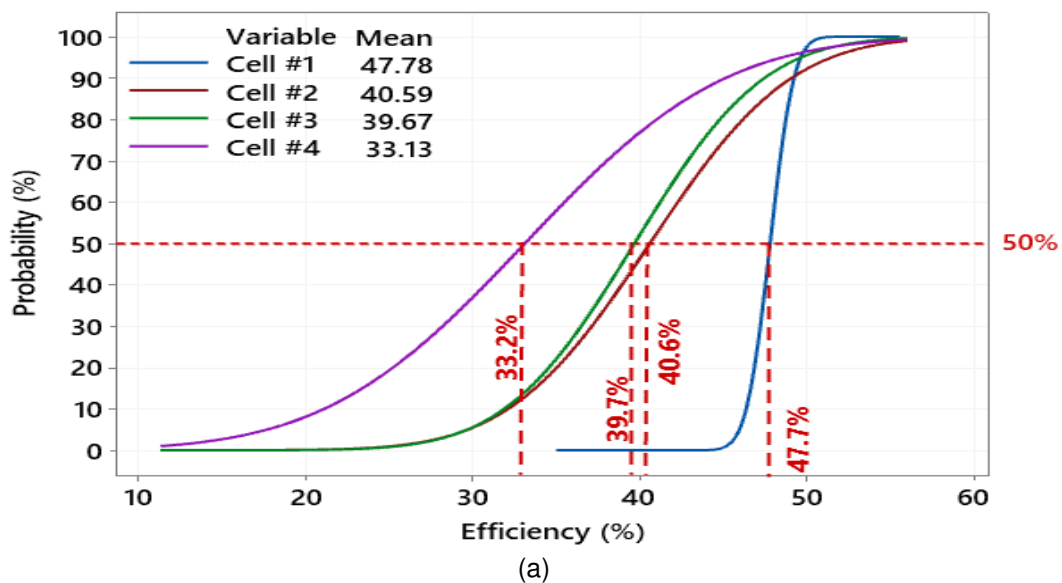


Fig. 10. Statistical results of the examined fuel cells (a) CDF profile, (b) Dendrogram profile.

## 5. Comparative Analysis

In Table III, we present a comparative study of our work vs. recently published studies on PEM fuel cells characterization and degradation, including [15], [20], and [31]. According to Pregelj *et al.* [20], they have presented the reliability results of a 3.0 kW PEM fuel cell. Results show that the internal DC-DC converter can lead to 96 W power consumption during the fuel cell operation, yet the efficiency is not reported. In contrast, Lie *et al.* [15] found that the efficiency could drop by 6% due to the varying voltage of a 3.0 kW fuel cell, close to our work's findings, 7.2%. However, as we presented in this work, they did not experiment with the degradation of the tested fuel cell at varying temperatures.

A recent study by Vichard *et al.* [31] shows that a 1.0 kW PEM fuel cell's efficiency can degrade by nearly 9% due to varying the temperature and the voltage simultaneously. However, this study did not explain the fuel cell efficiency in terms of the difference between varying the temperature or the stack voltage. Henceforth, we have presented a comprehensive study on the characterization and degradation of ordinarily utilized 3.2 kW PEM fuel cells with EVs. We found that varying the stack voltage could reduce the efficiency up to 7.2%. In comparison, there is an extra distinguished loss estimated at around 14.7% when the fuel cell's temperature is uncontrolled and remained as high as 95°C.

Table II  
Comparative analysis of our presented work with recently published work [15, 20 and 22]

Item	This work	Ref. [31]	Ref. [15]	Ref. [20]
Year of the study	2021	2020	2018	2017
Fuel cell type	PEM	PEM	PEM	PEM
Fuel cell application	EV	EV	EV	Industrial energy production
Maximum Rater Power (kW)	3.2	1.0	3.0	3.0
Pressure variations (bar)	0.1 to 0.5	No varying pressure	0.1 – 1.5	0.1 to 0.4
Short-circuit and purging routines	included	included	included	Included
Working testing cycle (hours)	4320	5000	991 and 1020	3
Degradation mechanism of varying voltage	100V down to 75V, maximum efficiency drops 7.2%	Six different cycles have been considered (temperature varying from 7°C to 30°C, and voltage varying from 19.8V to 17.5V). The conclusion suggests a 9% loss in efficiency, but, not sure if the drop results from the temperature or voltage variation	18V down to 12V, maximum efficiency drops 6%	47V down to 33V, efficiency drop is not recorded, only DC-DC converter efficiency drops by 96 W
Degradation mechanism of varying membrane temperature	95°C down to 50°C, maximum efficiency drops 14.7%		n/a	350°C down to 250°C, efficiency drop is not recorded, only DC-DC converter efficiency drops by 96 W

To summarize the results of this work, we have plotted the average efficiency of the fuel cells after operating for 180 days under different conditions (Fig. 11). The standard baseline (38%) for the efficiency of PEM fuel cells was also considered. A partial reduction in the efficiency is observed when the fuel cell is operating under high voltage, 100 V, for all tested membrane temperatures, between 55 to 95°C. However, when the fuel cell is running under lower voltages, 85 or 75 V, we found that if the membrane temperature is above 75°C, the efficiency drops significantly below the baseline of 38%.

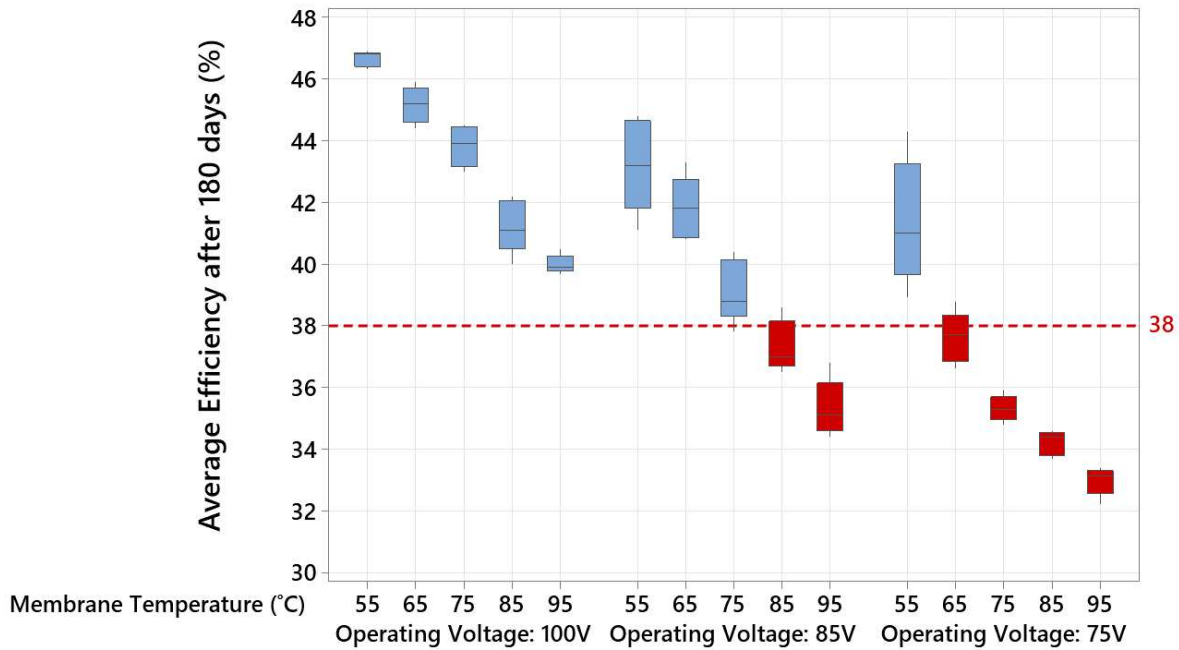


Fig. 11. Summary of the results while operating the fuel cell at different voltage and membrane temperatures.

## 6. Conclusion

In this paper, we have demonstrated our investigation on the stability and degradation of 3.2 kW PEM fuel cell, previously used in EV application. First, we have shown the electrical characteristics of the fuel cell during the normal operational mode, short-circuit condition, and purging routines. Here we have proven that when increasing the  $H_2$  pressure, the efficiency of the examined fuel cell gets higher, where the maximum observed efficiency is equal to 58%. Additionally, we have examined the four fuel cells of the same type while varying the fuel cell output voltage and the membrane temperature; this experimentation was managed over 180 consecutive days. We have found a minor reduction in efficiency when the fuel cell is operating under high voltage, 100 V, for all tested membrane temperatures, between 55 to 95°C. However, when the fuel cell is running under lower voltages, 85 or 75 V, we found that if the membrane temperature is above 75°C, the efficiency drops significantly, it was in the range between 33 to 37%. Thus, by far, our results support understanding the operational mechanisms of PEM fuel cells and their degradation response.

## 7. References

- [1] Sagar, A., Chugh, S., Sonkar, K., Sharma, A., & Kjeang, E. (2020). A computational analysis on the operational behaviour of open-cathode polymer electrolyte membrane fuel cells. *International Journal of Hydrogen Energy*, 45(58), 34125-34138.
- [2] Khalid, F., Dincer, I., & Rosen, M. A. (2016). Analysis and assessment of an integrated hydrogen energy system. *International Journal of Hydrogen Energy*, 41(19), 7960-7967.
- [3] Liu, J., Gao, Y., Su, X., Wack, M., & Wu, L. (2018). Disturbance-observer-based control for air management of PEM fuel cell systems via sliding mode technique. *IEEE Transactions on Control Systems Technology*, 27(3), 1129-1138.
- [4] Umaz, R. (2020). A Single Inductor Self-Startup Energy Combiner Circuit With Bioturbation Resilience in Multiple Microbial Fuel Cells. *IEEE Transactions on Circuits and Systems II: Express Briefs*, 67(12), 3227-3231.
- [5] Malik, F. R., Tieqing, Z., & Kim, Y. B. (2020). Temperature and hydrogen flow rate controls of diesel autothermal reformer for 3.6 kW PEM fuel cell system with autoignition delay time analysis. *International Journal of Hydrogen Energy*, 45(53), 29345-29355.
- [6] Gencoglu, M. T., & Ural, Z. (2009). Design of a PEM fuel cell system for residential application. *international journal of hydrogen energy*, 34(12), 5242-5248.
- [7] Yan, Y., Li, Q., Chen, W., Huang, W., & Liu, J. (2019). Hierarchical management control based on equivalent fitting circle and equivalent energy consumption method for multiple fuel cells hybrid power system. *IEEE Transactions on Industrial Electronics*, 67(4), 2786-2797.
- [8] Dhinish, M. (2019). 70% decrease of hot-spotted photovoltaic modules output power loss using novel MPPT algorithm. *IEEE Transactions on Circuits and Systems II: Express Briefs*, 66(12), 2027-2031.
- [9] Hong, T., Geng, Z., Qi, K., Zhao, X., Ambrosio, J., & Gu, D. (2020). A Wide Range Unidirectional Isolated DC-DC Converter for Fuel Cell Electric Vehicles. *IEEE Transactions on Industrial Electronics*, 68(7), 5932-5943.
- [10] Slah, F., Mansour, A., Hajer, M., & Faouzi, B. (2017). Analysis, modeling and implementation of an interleaved boost DC-DC converter for fuel cell used in electric vehicle. *International journal of hydrogen energy*, 42(48), 28852-28864.
- [11] Umaz, R. (2019). A power management system for microbial fuel cells with 53.02% peak end-to-end efficiency. *IEEE Transactions on Circuits and Systems II: Express Briefs*, 67(11), 2592-2596.
- [12] Li, Q., Yang, W., Yin, L., & Chen, W. (2020). Real-time implementation of maximum net power strategy based on sliding mode variable structure control for proton-exchange membrane fuel cell system. *IEEE Transactions on Transportation Electrification*, 6(1), 288-297.
- [13] Xing, Y., Na, J., & Costa-Castello, R. (2019). Real-time adaptive parameter estimation for a polymer electrolyte membrane fuel cell. *IEEE Transactions on Industrial Informatics*, 15(11), 6048-6057.
- [14] Bankupalli, P. T., Ghosh, S., Kumar, L., Samanta, S., & Jain, S. (2019). Operational adaptability of PEM fuel cell for optimal voltage regulation with maximum power extraction. *IEEE Transactions on Energy Conversion*, 35(1), 203-212.
- [15] Liu, H., Chen, J., Hissel, D., & Su, H. (2018). Short-term prognostics of PEM fuel cells: A comparative and improvement study. *IEEE Transactions on Industrial Electronics*, 66(8), 6077-6086.
- [16] Lindahl, P. A., Shaw, S. R., & Leeb, S. B. (2018). Fuel cell stack emulation for cell and hardware-in-the-loop testing. *IEEE Transactions on Instrumentation and Measurement*, 67(9), 2143-2152.
- [17] Lee, S., Han, G., Kim, T., Yoo, Y. S., Jeon, S. Y., & Bae, J. (2020). Connected evaluation of polymer electrolyte membrane fuel cell with dehydrogenation reactor of liquid organic hydrogen carrier. *International Journal of Hydrogen Energy*, 45(24), 13398-13405.
- [18] Ligen, Y., Vrabel, H., & Girault, H. (2020). Energy efficient hydrogen drying and purification for fuel cell vehicles. *International Journal of Hydrogen Energy*, 45(18), 10639-10647.
- [19] Javaid, U., Mehmood, A., Arshad, A., Imtiaz, F., & Iqbal, J. (2020). Operational efficiency improvement of PEM fuel cell—A sliding mode based modern control approach. *IEEE Access*, 8, 95823-95831.
- [20] Pregelj, B., Debenjak, A., Dolanc, G., & Petrovčič, J. (2017). A diesel-powered fuel cell APU—reliability issues and mitigation approaches. *IEEE Transactions on Industrial Electronics*, 64(8), 6660-6670.
- [21] Gong, X., Dong, F., Mohamed, M. A., Abdalla, O. M., & Ali, Z. M. (2020). A secured energy management architecture for smart hybrid microgrids considering PEM-fuel cell and electric vehicles. *IEEE Access*, 8, 47807-47823.

- [22] Valdez-Resendiz, J. E., Sanchez, V. M., Rosas-Caro, J. C., Mayo-Maldonado, J. C., Sierra, J. M., & Barbosa, R. (2017). Continuous input-current buck-boost DC-DC converter for PEM fuel cell applications. *International Journal of Hydrogen Energy*, 42(51), 30389-30399.
- [23] Maleki, A. (2021). Optimal operation of a grid-connected fuel cell based combined heat and power systems using particle swarm optimisation for residential sector. *International Journal of Ambient Energy*, 42(5), 550-557.
- [24] Mohamed, M. A., Abdullah, H. M., El-Meligy, M. A., Sharaf, M., Soliman, A. T., & Hajjiah, A. (2021). A novel fuzzy cloud stochastic framework for energy management of renewable microgrids based on maximum deployment of electric vehicles. *International Journal of Electrical Power & Energy Systems*, 129, 106845.
- [25] Rezaei, M., Khalilpour, K. R., & Mohamed, M. A. (2021). Co-production of electricity and hydrogen from wind: A comprehensive scenario-based techno-economic analysis. *International Journal of Hydrogen Energy*, 46(35), 18242-18256.
- [26] Rizvandi, O. B., Miao, X. Y., & Frandsen, H. L. (2021). Multiscale modeling of degradation of full solid oxide fuel cell stacks. *International Journal of Hydrogen Energy*, 46(54), 27709-27730.
- [27] Hahn, S., Braun, J., Kemmer, H., & Reuss, H. C. (2021). Optimization of the efficiency and degradation rate of an automotive fuel cell system. *International Journal of Hydrogen Energy*, 46(57), 29459-29477.
- [28] Vasilyev, A., Andrews, J., Dunnett, S. J., & Jackson, L. M. (2021). Dynamic reliability assessment of PEM fuel cell systems. *Reliability Engineering & System Safety*, 210, 107539.
- [29] Dhimish, M., Mather, P., & Holmes, V. (2019). Novel photovoltaic hot-spotting fault detection algorithm. *IEEE Transactions on Device and Materials Reliability*, 19(2), 378-386.
- [30] Dhimish, M., Schofield, N., & Attya, A. (2020). Insights on the Degradation and Performance of 3000 Photovoltaic Installations of Various Technologies Across the United Kingdom. *IEEE Transactions on Industrial Informatics*, 17(9), 5919-5926.
- [31] Vichard, L., Harel, F., Ravey, A., Venet, P., & Hissel, D. (2020). Degradation prediction of PEM fuel cell based on artificial intelligence. *International Journal of Hydrogen Energy*, 45(29), 14953-14963.